Available online at www.sciencedirect.com

ScienceDirect

Mendeleev Commun., 2019, **29**, 382–384

Mendeleev Communications

CO_2 hydrogenation on Fe-based catalysts doped with potassium in gas phase and under supercritical conditions

Yana A. Pokusaeva,*[a] Aleksey E. Koklin,[a] Valery V. Lunin[a,b] and Victor I. Bogdan*[a,b]

[a] *N. D. Zelinsky Institute of Organic Chemistry, Russian Academy of Sciences, 119991 Moscow, Russian Federation. E-mail: vibogdan@gmail.com, yana_pokusaeva@inbox.ru*

[b] *Department of Chemistry, M. V. Lomonosov Moscow State University, 119991 Moscow, Russian Federation*

DOI: 10.1016/j.mencom.2019.07.007

New catalysts FeK/Sibunit and FeCuK/Sibunit were prepared and applied for the CO_2 hydrogenation in the temperature range of 250–400 °C and under the pressures of 1, 20 and 85 atm. The reverse water gas shift reaction prevailed under the atmospheric pressure (*i.e.*, CO_2 was selectively converted into CO), while the formation of C_1–C_{12} hydrocarbons occurred under the increased pressures. The Cu-containing catalyst exhibited the higher activity and selectivity towards C_1–C_{12} hydrocarbons.

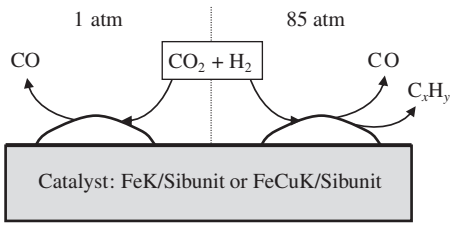

Decreases in the amount of CO_2 emissions are a challenge for modern science since it is the main green-house gas having a significant impact on the global climate change. Carbon capture and storage technologies were developed in response to this challenge. Novel approaches to trap carbon dioxide and store it in special geological reservoirs underground[1] are being developed all over the world. Carbon capture and utilization is another technology, which is more attractive since carbon dioxide can be considered as an inexpensive renewable raw material for the synthesis of valuable chemicals. One of the CO_2 chemical recycling methods is its catalytic hydrogenation into fuels such as methane and other hydrocarbons.[2,3] Although H_2 remains quite expensive for the practical implementation of this technology, hydrogen energy is constantly evolving, which consequently results in a trend of decreasing hydrogen prices. Hydrogen can be produced by various methods including water electrolysis, biophotolysis, fermentation processes, and gasification of biomass in supercritical water.[4–8]

Iron-based catalysts have already demonstrated their activity in the reverse water-gas shift (RWGS) reaction, Fischer–Tropsch synthesis, and CO_2 hydrogenation.[2,9,10] To attain high activity and stability of these catalysts, the addition of other metals and promoters tuning the surface electronic or structural properties is required. Bimetallic Fe–Cu catalysts are commonly applicable to the hydrogenation of carbon oxides into hydrocarbons. Copper catalysts are also active in the RWGS reaction but do not catalyze CO_2 methanation.[2] Doping with potassium enhances the catalytic activity of catalysts in the CO_2 hydrogenation.[10,11]

Carbon dioxide hydrogenation was investigated under supercritical conditions.[12–17] A supercritical media may enhance the catalyst activity and productivity, prolonging its lifetime. These advantages can be maintained by unique properties of the supercritical media, such as gas-like diffusion properties and liquid-like density.[18]

Here we report preliminary results of our ongoing project aimed at investigations of the supercritical effects on the catalytic efficiency of Fe-based catalysts in CO_2 hydrogenation. Thus, carbon dioxide hydrogenation was carried out at 300–400 °C and 1, 20 and 85 atm, where the first two pressures are related to the gas phase, while 85 atm corresponds to supercritical conditions. Although few H_2 molecules are needed for the production of a hydrocarbon from one CO_2 molecule, the equimolar mixture of CO_2 and H_2 was selected in this work since the density of the reaction medium is very important for carrying out catalytic reactions under supercritical conditions. Critical parameters of this mixture calculated with REFPROP 8.0 were 169 K and 4.5 MPa. The mixture density decreases with raising the CO_2 : H_2 ratio (up to 1 : 2 or 1 : 3), which could adversely affect the lifetime and activity of catalysts.

Catalysts Fe(20%)K(1%)/Sibunit and Fe(20%)Cu(1%)K(1%)/Sibunit (wt%) were prepared *via* the triple incipient wetness impregnation. Sibunit carbon material was used as a support.[†] Application of activated carbon supports may be limited by a high content of sulfur and other minerals, micropore structure, and low stability. Commercially available mesoporous carbon material Sibunit was selected due to its mechanical and thermal stability, chemical purity, and high sorption capacity.[19] XRD patterns of FeCuK/Sibunit and FeK/Sibunit catalysts are available in Online Supplementary Materials (Figure S1).[‡] The diffraction peaks can be attributed to the magnetite iron oxide Fe_3O_4 (JCPDS card no. 82-1533). Other phases containing potassium and copper were not detected by XRD probably due to their low concentration.

[†] Sibunit (manufactured by Tomsk NIIPN, granule sizes of 1–2 mm, surface area of 340 $m^2\ g^{-1}$) was dried at 110 °C in air for 6 h before the impregnation. Solutions of metal precursors were prepared by dissolving the nitrates of corresponding metals [$Fe(NO_3)_3 \cdot 9H_2O$, $Cu(NO_3)_2 \cdot 6H_2O$, and KNO_3] in distilled water. The calculated concentrations of loading metals were 20, 1 and 1 wt% for Fe, Cu and K, respectively. After the impregnation, the catalysts were dried at 80 °C for 6 h and then calcined under argon flow at 450 °C for 4 h.

[‡] X-ray diffraction data were acquired on a DRON3 diffractometer (CuKα radiation) in the region of 2θ = 20–60° at the scanning rate of 1 deg min^{-1}.

Table 1 CO_2 hydrogenation over FeCuK/Sibunit and FeK/Sibunit (CO_2 : H_2 ratio of 1:1).

Catalyst	*T*/°C	*P*/atm	CO_2 conversion (%)	Selectivity (%)	
				CO	C_xH_y
FeCuK/Sibunit	350	1	8	100	0
	400		21	100	0
	300	85	12	65	35
	350		15	50	50
	400		17	53	47
FeK/Sibunit	300	1	3	100	0
	350		13	100	0
	400		24	100	0
	350	20	12	93	7
	300	85	7	73	27
	350		12	76	24
	400		17	72	28

Average size of magnetite particles calculated according to the Scherrer equation was 12–15 nm. According to TEM results (Figure S2), the average size of species was 12–13 nm.

The catalytic activity in the CO_2 hydrogenation was estimated in a flow-type fixed-bed stainless steel reactor (250–400 °C; 1, 20 and 85 atm).[§]

Total reaction (3) of catalytic CO_2 hydrogenation into hydrocarbons on Fe-based catalysts can be represented as a two-step process comprising of the RWGS reaction (1) and consequent Fischer–Tropsch synthesis (2).

$$x\mathrm{CO_2} + x\mathrm{H_2} = x\mathrm{CO} + x\mathrm{H_2O} \quad (1)$$

$$x\mathrm{CO} + (y/2 + x)\mathrm{H_2} = \mathrm{C}_x\mathrm{H}_y + x\mathrm{H_2O} \quad (2)$$

$$x\mathrm{CO_2} + (y/2 + 2x)\mathrm{H_2} = \mathrm{C}_x\mathrm{H}_y + 2x\mathrm{H_2O} \quad (3)$$

Experimental data on the reduction of carbon dioxide with hydrogen in gas phase (at 1 and 20 atm pressure) and under supercritical conditions (85 atm) are given in Table 1. At 250 °C, the CO_2 conversion was negligible at 1 and 20 atm and very low (less than 3%) at 85 atm.

Direction of the process and the distribution of products were significantly affected by the pressure in the reaction mixture. The RWGS reaction prevailed in the case of atmospheric pressure, *i.e.* carbon dioxide was selectively converted into carbon monoxide, and only at temperatures above 350 °C, trace amounts of methane and light hydrocarbons (C_1–C_3) were formed. The effect of pressure increased up to 20 atm was investigated on FeK/Sibunit. Hydrocarbons ratio growth was observed upon the elevated pressure. When the pressure was increased up to 85 atm at 350 °C (supercritical phase), the selectivity towards CO was reduced to 50%. Thus, a mixture of hydrocarbon products was obtained with selectivity of up to 50% (see Tables 1 and 2). Formation of linear and iso-C_1–C_{12} hydrocarbons and light olefins was observed for the both considered catalysts.

The pressure does not have any measurable effect on the conversion of a CO_2/H_2 mixture, *i.e.* on the thermodynamic equilibrium of the RWGS. The first step of tandem process was considered, which determines the overall CO_2 conversion.[20] However, at an increased pressure, the equilibrium in the formation of long-chain hydrocarbons (C_{5+}) increases in agreement with the Fischer–Tropsch reaction mechanism (polymerization–condensation).

[§] Feed mixture containing CO_2 and H_2 at the molar ratio of 1 : 1 was fed at a flow rate of 80 ml min^{-1} (NTP). Carbon dioxide was fed into the reactor with high-pressure pump, and hydrogen was introduced with a Bronkhorst mass flow controller. Catalyst load was 2.0 cm^3 (1.5 g). The pressure was maintained by a back pressure valve. Products were analyzed by gas chromatography with a thermal conductivity detector (TCD) on Porapak Q and CaA packed columns and a flame ionization detector (FID) on a Thermo TR-5MS capillary column.

Table 2 Products selectivity and chain growth probability (α) in CO_2 hydrogenation at 350–400 °C and 85 atm (CO_2 : H_2 = 1 : 1).

Catalyst	*T*/°C	Selectivity (%)				α
		CO	CH_4	C_2–C_4	C_{5+}	
FeCuK/Sibunit	350	50	11	21	18	0.58
	400	53	13	19	15	0.56
FeK/Sibunit	350	76	6	10	8	0.57
	400	72	7	11	10	0.59

Under the same conditions, the copper-containing FeCuK/Sibunit catalyst demonstrated higher activity and selectivity towards C_1–C_{12} as compared to FeK/Sibunit. In the presence of Fe–Cu catalyst, the hydrocarbon formation has been already started at 300 °C with CO_2 conversion of 12% and selectivity of 35%. It may be related to the reduction of Fe species facilitated by Cu.[21]

Figure 1 shows the distribution of hydrocarbon products for used catalysts. In both cases, the major products were light alkanes and C_1–C_4 olefins (more than 60% of all hydrocarbons). The fraction of heavier hydrocarbon products exponentially decreases with raising the number of carbon atoms.

Formation of hydrocarbon products C_xH_y in the catalytic CO_2 hydrogenation can be described by the Anderson–Schulz–Flory distribution law analogously to the case of the Fischer–Tropsch reaction with CO and H_2 as a feedstock (Figure 2). The values of chain growth probability α (see Table 2) were calculated from the plots of $\log(W_n/n)$ *vs.* n, where W_n is the hydrocarbon concentration, and n is the number of carbon atoms in a hydrocarbon molecule. In the temperature range from 300 to 400 °C, the values α were close (~0.6) for both catalysts.

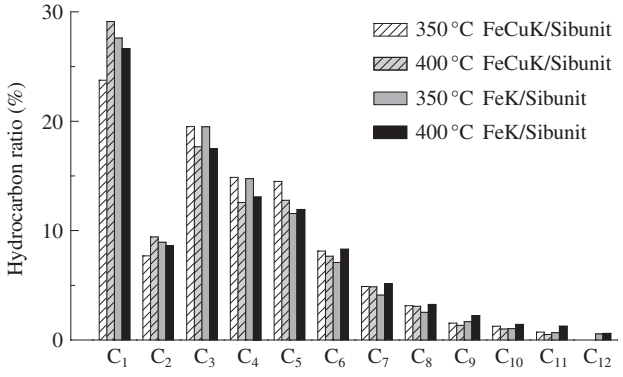

Figure 1 Distribution of hydrocarbon products of CO_2 hydrogenation at 350 and 400 °C on the prepared catalysts (85 atm, CO_2 : H_2 ratio of 1 : 1).

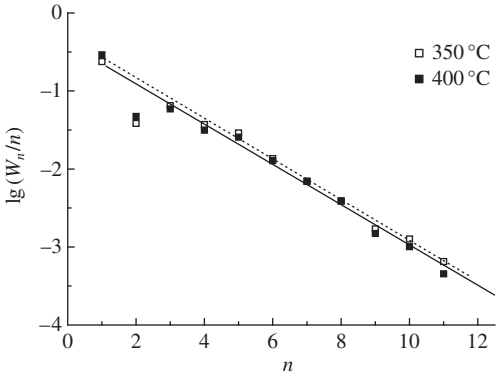

Figure 2 C_1–C_{12} hydrocarbon products distribution (CO_2 hydrogenation over FeCuK/Sibunit at 350 and 400 °C, 85 atm pressure, CO_2 : H_2 ratio of 1 : 1).

A deviation in the products distribution from the Anderson–Schulz–Flory law was observed as a decreased amount of C_2 hydrocarbons. However, such variation in the product distribution is quite common.[22] Ethane and ethylene can initiate the growth of a new chain or be incorporated in other growing hydrocarbon chains resulting in a lower fraction of C_2 products than that expected according to the normal Anderson–Schulz–Flory distribution.

In conclusion, the new synthesized Fe-based catalysts were active in the CO_2 hydrogenation into hydrocarbons. Their doping with copper caused a positive effect on the yield of hydrocarbons. At the temperature of 300–400 °C and atmospheric pressure, carbon monoxide was the only product, while the formation of hydrocarbons was observed at 20 atm, and the best selectivity towards hydrocarbons (about 50%) was in the case of pressure of 85 atm. The study will be continued to reveal the effects of other reaction parameters, such as $CO_2 : H_2$ ratio, *etc*.

Online Supplementary Materials

Supplementary data associated with this article can be found in the online version at doi: 10.1016/j.mencom.2019.07.007.

References

1 A. Scibioh and B. Viswanathan, *Carbon Dioxide to Chemicals and Fuels*, Elsevier, Amsterdam, 2018.
2 W. Wang, S. Wang, X. Ma and J. Gong, *Chem. Soc. Rev*., 2011, **40**, 3703.
3 G. Centi and S. Perathoner, *Catal. Today*, 2009, **148**, 191.
4 D. B. Levin, L. Pitt and M. Love, *Int. J. Hydrogen Energy*, 2004, **29**, 173.
5 S. Manish and R. Banerjee, *Int. J. Hydrogen Energy*, 2008, **33**, 279.
6 Y. Guo, S. Z. Wang, D. H. Xu, Y. M. Gong, H. H. Ma and X. Y. Tang, *Renewable Sustainable Energy Rev*., 2010, **14**, 334.
7 T. Yoshida, Y. Oshima and Y. Matsumura, *Biomass Bioenergy*, 2004, **26**, 71.
8 V. I. Bogdan, A. V. Kondratyuk, A. E. Koklin and V. V. Lunin, *Russ. J. Phys. Chem., B*, 2017, **11**, 1207 [*Sverkhkriticheskie Flyuidy. Teoriya i Praktika*, 2016, **11** (4), 80].
9 P. H. Choi, K.-W. Jun, S.-J. Lee, M.-J. Choi and K.-W. Lee, *Catal. Lett*., 1996, **40**, 115.
10 S.-R. Yan, K.-W. Jun, J.-S. Hong, M.-J. Choi and K.-W. Lee, *Appl. Catal., A*, 2000, **63**, 194.
11 N. Boreriboon, X. Jiang, C. Song and P. Prasassarakich, *Top. Catal*., 2018, **61**, 1551.
12 I. Omae, *Catal. Today*, 2006, **115**, 33.
13 V. I. Bogdan and L. M. Kustov, *Mendeleev Commun*., 2015, **25**, 446.
14 V. I. Bogdan, A. E. Koklin, S. A. Nikolaev and L. M. Kustov, *Top. Catal*., 2016, **59**, 1104.
15 P. G. Jessop, *J. Supercrit. Fluids*, 2006, **38**, 211.
16 B. Tidona, C. Koppold, A. Bansode, A. Urakawa and P. R. von Rohr, *J. Supercrit. Fluids*, 2013, **78**, 70.
17 N. D. Evdokimenko, A. L. Kustov, K. O. Kim, M. S. Igonina and L. M. Kustov, *Mendeleev Commun*., 2018, **28**, 147.
18 A. Baiker and R. Wandeler, *CATTECH*, 2000, **4**, 128.
19 V. F. Surovikin, G. V. Plaxin, V. A. Semikolenov, V. A. Likholobov and I. J. Tiunova, *Patent US 4978649 A*, 1989.
20 L. Torrente-Murciano, D. Mattia, M. D. Jones and P. K. Plucinski, *J. CO_2 Util*., 2014, **6**, 34.
21 D. B. Bukur, D. Mukesh and S. A. Patel, *Ind. Eng. Chem. Res*., 1990, **29**, 194.
22 L. S. Glebov and G. A. Kliger, *Russ. Chem. Rev*., 1994, **63**, 185 (*Usp. Khim*., 1994, **63**, 192).

Received: 23rd November 2018; Com. 18/5745